# Reconstruction of a distribution from a finite number of moments with an adaptive spline-based algorithm

L.G.M. de Souza [a], G. Janiga [a], V. John [b,c], D. Thévenin [a,*]

[a] Laboratory of Fluid Dynamics and Technical Flows, University of Magdeburg "Otto von Guericke", Germany
[b] Weierstrass Institute for Applied Analysis and Stochastics, Berlin, Germany
[c] Free University of Berlin, Department of Mathematics and Computer Science, Germany

## A B S T R A C T

An adaptive algorithm suitable for reconstructing a distribution when knowing only a small number of its moments is presented. This method elaborates on a previous technique presented in John et al. (2007), but leads to many advantages compared with the original algorithm. The so-called "finite moment problem" arises in many fields of science, but is particularly important for particulate flows in chemical engineering. Up to now, there is no well-established algorithm available to solve this problem. The examples considered in this work come from crystallization processes. For such applications, it is of crucial interest to reconstruct the particle size distributions (PSD) knowing only a small number of its moments, obtained mostly from numerical simulations or from advanced experiments, but without any a priori knowledge concerning the shape of this PSD. This was already possible in many cases with the original algorithm of John et al. (2007), but complex shapes could not be identified appropriately. The key of the advanced algorithm is the adaptive criterion for positioning dynamically the nodes in an appropriate manner. It turns out that the adaptive algorithm shows considerable improvements in the reconstruction of distributions with a quickly changing curvature or for non-smooth distributions. Since such configurations are quite often found in practice, the new algorithm is more widely applicable compared with the original method.

## 1. Introduction

The problem of reconstructing a scalar-valued function $f(t, x)$ from a finite number of its moments, the so-called "finite moment problem", arises in many scientific and technical applications as described in John et al. (2007). This situation has not changed; the interested reader is therefore referred to the literature cited in John et al. (2007) to find application examples for image processing, magnetic imaging, molecular physics or chemical engineering.

The $i$-th moment $\mu_i(t)$ of the function $f(t,x) : [0, t_{final}) \times [0, \infty) \rightarrow \mathbb{R}$ depending on time and on a one-dimensional, so-called internal coordinate $x$ (typically, a length scale) is classically defined by

$$\mu_i(t) = \int_0^\infty x^i f(t,x)\,dx, \quad i = 0, 1, 2, \dots. \tag{1}$$

Since a majority of practical applications still only considers mono-variate problems at present, the developed formulation will be restricted to the case of a single internal coordinate $(x)$. Bivariate populations will be the subject of future work.

From the mathematical point of view, the finite moment problem is a severely ill-posed problem. It has been studied in the mathematical literature almost exclusively from the theoretical point of view (see again John et al., 2007 for a review of the most important results). In principle, there is no unique solution for this problem and all moments up to infinity should be known to reconstruct the function. The issue of isomomental distributions (i.e., distributions having the same moments while being different) has been considered extensively for instance in Wright (2000) and White (1990).

Nevertheless, there are usually constraints on the domain and on the range of $f(t, x)$ due to the underlying physics of the application. A typical example is the reconstruction of particle size distributions (PSD) when considering particulate processes like crystallization, precipitation, etc. The particle size ($x$ coordinate) is always positive, and there is always a maximal possible size, at most the reactor size, usually even much smaller. Thus, the domain spanned in the $x$-direction by $f(t, x)$ is only an interval within the positive real numbers. Furthermore, a PSD should have only non-negative values, hence the range of $f(t, x)$ is only a subset of the non-negative real numbers. Even if these limitations sound trivial from an engineering point of view, they are indeed

* Corresponding author.
  E-mail addresses: Luis.MedeirosDeSouza@student.uni-magdeburg.de (L.G.M. de Souza), janiga@ovgu.de (G. Janiga), john@wias-berlin.de (V. John), thevenin@ovgu.de (D. Thévenin).

sufficient from a mathematical point of view to simplify tremendously the complexity of the finite moment problem as recognized also for instance by Strumendo and Arastoopour (2008). The uniqueness of the reconstruction in the case all moments are known is discussed in Appendix A. However, different distributions having the same first moments are still possible.

Usually, the moments $\mu_i$ associated with the distribution are determined using numerical simulations or advanced experimental techniques. Note, however, that corresponding measurements are extremely difficult, in particular if a high accuracy is required, as documented for example in Allen (1997). As a consequence, only very few moments are usually determined experimentally, mostly in an indirect manner. In practice, only the mean particle size and the particle number concentration can be measured with a relatively high accuracy, even if some set-ups deliver an estimation of the complete PSD (e.g., Bałdyga and Orciuch, 2001; Marchisio et al., 2002). This demonstrates the importance of a robust reconstruction method that is able to deliver a good approximation of the underlying distribution with only limited information input.

The situation is not quite as difficult when the moments are determined from numerical simulations. Indeed, very popular numerical techniques like method of moments (MOM), Quadrature method of moments (QMOM) and direct quadrature method of moments (DQMOM; see Marchisio and Fox, 2005 for more information on these techniques) directly deliver the moment values. In principle, it is possible to consider as many moments as the user wishes. But the cost of the numerical simulation of course increases rapidly when considering more moments. Furthermore, the mathematical system becomes very badly conditioned for higher-order moments. As a consequence, results found in recent publications deliver a larger but still limited number of moments. For instance, two (Schwarzer et al., 2006), three (Diemer and Olson, 2002), four (Wei et al., 2001), five (Öncül et al., 2009) or even for test purposes up to eight moments (Fan et al., 2004) have been considered for coupled simulations involving particles in a turbulent flow.

For practical engineering purposes, the usual method for reconstructing a function from a small number of its moments is based on an a priori knowledge of the solution. Using this information (e.g., a Gauss shape, or a Poisson distribution), a strong ansatz is made for the shape of $f(t, x)$ and the known moments are just used to fit parameters in this ansatz. This fitting is a fast and very easy computation. Nevertheless, this approach is restricted to functions with simple shapes. Even more troublesome is the fact that one needs in principle to know the solution before one can get it back, which is obviously not very satisfactory in general (see John et al., 2007 for a more detailed discussion of the advantages and drawbacks of this approach). A direct reconstruction is only possible if the number of known moments is equal to the number of parameters in the ansatz. As an additional difficulty, the shape of the function needed to reconstruct is often time-dependent in practical applications, $f(t, x)$. It is then not clear if the presumed shape is suitable for all times.

Further possible techniques to solve the finite moment problem have been already reviewed in John et al. (2007). For the sake of brevity, the corresponding analysis is not repeated here, so that only new approaches are discussed in what follows. One notable exception concerns the maximum entropy method (MEM). Before introducing the spline-based reconstruction in John et al. (2007), MEM was clearly the best possible method for reconstructing the PSD and it is still an interesting alternative today, so that it deserves a renewed discussion. Recent publications using MEM for reconstructing a distribution can be found in

particular in Abramov (2007) and Bandyopadhyay et al. (2005). In order to compute a reconstruction, MEM starts from a so-called prior distribution chosen by the user and applies a finite number of explicit constraints. As a consequence, the shape of the reconstruction is not completely prescribed, but the results still depend on the choice of the prior distribution (sometimes also called sample distribution). Theoretically, as the number of available moments grows, the results of MEM should become more and more independent from the prior distribution. However, improper priors still influence strongly the results of MEM, as shown for example in Kass and Wasserman (1996) and Scales and Tenorio (2001). Furthermore, only a limited number of moments are known in practice, leading to an even larger influence of the sample distribution on the final result.

Improved reconstruction methods derived from MEM can be found, in particular the minimum relative entropy (MRE) method (see for example Woodbury, 2004). The MRE is superior to MEM in several aspects. However, the results obtained with MRE still depend on the choice of a prior, just like MEM. It has been furthermore shown that, if the prior is chosen to be a smooth function (which is almost always done in practice), the results of MRE or MEM will be necessarily a smooth function too (Woodbury, 2004). Therefore, it is extremely difficult to reconstruct non-smooth distributions with this technique.

To finally conclude on entropy methods, they are indeed quite attractive and a considerable amount of information can be found in the literature. They request nevertheless either a good a priori knowledge of the distribution that must be reconstructed (approximate shape, smooth or non-smooth evolution) and/or a large number of moments. Our objective in the present work is somewhat different: to propose a robust method able to deliver an acceptable reconstruction independently from any initial guess and with only a limited number of known moments.

After the publication of the survey in John et al. (2007), another reconstruction algorithm was introduced in Alopaeus et al. (2008). Similar to our spline-based approach, this method does not constrain directly the shape of the distribution to be reconstructed. The technique described in Alopaeus et al. (2008) assumes that good estimates of the function to reconstruct are known at some isolated points. A piecewise linear interpolation between these points gives an approximation of the function, the so-called raw solution. The possible negative oscillations of this raw solution are simply cut off, which simultaneously gives an assumed range for the raw solution. In this way, a first approximation of the solution is obtained, which might lead to moments completely different from the known values. The final step of the reconstruction method consists in a minimization of these differences in a least squares sense by a proper scaling of the abscissas and ordinates of the initial approximation. The method introduced in Alopaeus et al. (2008) is in principle attractive for a reconstruction process starting from a computer simulation relying by itself on a moment-based method. It cannot be applied directly to other cases such as to a reconstruction based on experimentally determined values.

Strumendo and Arastoopour (2008) have proposed the alternative Finite size domain Complete set of trial functions Method of Moments (FCMOM). As in the present formulation, this method uses explicitly the fact that the $x$-domain on which the distribution must be reconstructed is bounded. Up to now, FCMOM has been successfully employed to describe the evolution of particulate systems, but has not been used for coupled simulations involving non-homogeneous external coordinates such as particles in a complex turbulent flow. This is clearly our own target application. Furthermore, the examples published up to now with FCMOM employ a large number of moments (typically 10). Therefore, the purpose of our reconstruction

technique appears to be quite different and FCMOM will not be discussed further here.

In John et al. (2007), a reconstruction approach was presented, which does not require any information on the shape to be reconstructed nor on the spatial extent ($x$ coordinate) of the function $f(t, x)$. The unknown function is represented by a spline defined on an underlying grid. An arbitrary number of moments can be used for the reconstruction, and the real $x$-domain is identified iteratively during the reconstruction.

The standard approach presented in John et al. (2007) was very successful for many different distributions, but suffered from major drawbacks:

1. it cannot really reconstruct non-smooth distributions;
2. even smooth functions are not always well reconstructed, in particular when they involve several peaks (lack of generality).

As a whole, this means that the original procedure is not general enough. While the first and third PSD examples are well reconstructed (see Figs. 8 and 10 in John et al., 2007), the second and the fourth ones are not really acceptable (see Figs. 9 and 11). This is not a surprise for the fourth example (non-smooth distribution), but even the second, relatively simple example (smooth distribution involving two peaks) could not be reconstructed very properly. An in-depth analysis of the spline-based reconstruction process has shown that a tremendous progress could be obtained by placing the underlying grid points in an optimal manner. Working with an equidistant grid, such as in the original formulation, is not a good idea. Exhaustive tests using a manual positioning of the nodes have been carried out and the idea for the automatic algorithm emerged from these "trial and error" tests. Thus, the present paper will introduce a major improvement: the reconstruction will employ a non-equidistant grid, dynamically adapted during the reconstruction process. The main issue consists in finding appropriate criteria for an optimal distribution of the grid points. This issue will be addressed and numerical results will be presented, showing the large superiority of the improved method compared with the original one, particularly for non-smooth or multi-peak PSDs.

## 2. The adaptive spline-based reconstruction algorithm

The original spline-based reconstruction algorithm has been presented in detail in John et al. (2007). In principle, this presentation was already valid for non-equidistant grids. For this reason, we will limit ourselves here to the description of the most important features of this algorithm and to its extension concerning the adaptive distribution of the nodes. The chosen examples still come from crystallization reactors, since determining the correct PSD is a particularly important issue in this case as noted for example in Mersmann (2001).

The reconstruction of particle size distributions as found in process engineering is our major purpose, in particular for non-homogeneous conditions in space. Thus, the usual constraints on the domain (internal coordinate $x$) and the range of the function $f(t, x)$ to be reconstructed apply as described in the introduction: the particle size is positive and bounded; the PSD $f$ is non-negative everywhere.

Let the first $L$ moments of $f(t, x)$ be given at some time. An initial interval $[a, b]$, which should contain the real range of $f(t, x)$, is divided into $n$ sub-intervals $[x_i, x_{i+1}]$, $i=1,\ldots,n$, with $a = x_1 < x_2 < \cdots < x_{n+1} = b$. As in John et al. (2007), splines (piecewise polynomials with compatibility conditions at the nodes $x_i$, $i=2,\ldots,n$) of order 3 are used in the reconstruction. For such a cubic spline, there are in each interval 4 unknown

coefficients of the cubic polynomial leading altogether to $4n$ unknowns. From the boundary conditions at $x_1$ and $x_{n+1}$ and the compatibility conditions at $x_i$, $i=2,\ldots,n$, one obtains $3n + 3$ equations. The missing $L = n - 3$ equations come from the known moments of $f(t, x)$. Altogether, one has to solve in the spline-based reconstruction with cubic splines linear systems of equations of size $4n \times 4n$.

The spline-based reconstruction algorithm from John et al. (2007) is an iterative process. Given a mesh $x_1 < x_2 < \cdots < x_{n+1}$, one iteration looks as follows:

1. *Solve the resulting linear system of equations.*
2. *Check if the interval $[x_1, x_{n+1}]$ for computing the reconstruction can be reduced*: This step is crucial for finding a good interval, which contains the real domain of $f(t, x)$. In this step, the absolute values of the current reconstruction in the sub-intervals at the boundaries $[x_1, x_2]$, $[x_n, x_{n+1}]$, are compared with the maximal value of the current reconstruction. If, for instance, the values in $[x_1, x_2]$ are negligibly small compared with the maximal value, the new left boundary for the reconstruction is set to be $x_1 := (x_1 + x_2)/2$. The same procedure is performed for the right boundary. If the interval has changed, the nodes are redistributed in an equidistant manner. Go to step 1.
3. *Regularize the solution of the linear system of equations*: If there is no recommendation to reduce the interval in step 2, but the reconstruction has local values which are exceedingly negative, the solution of the linear system will be regularized. This is done by removing subsequently the smallest singular values of the system matrix. After each such removal, it is checked again if the interval for the reconstruction can be reduced, i.e., step 2 is performed.

The algorithm stops if all values in the nodes and in the midpoints of the sub-intervals are almost non-negative and if no reduction of the interval for the reconstruction is recommended.

The regularization of the linear system removes first the smoothness of the second derivative in the nodes. Thus, the recommended reconstruction will be often not twice differentiable (the second order derivative of the PSD is a piecewise linear but discontinuous function). This is not an issue for engineering purposes.

The procedure for an adaptive redistribution of the nodes needs some starting guess about the shape of the expected solution. This is a classical requirement for adaptive methods, e.g., for the solution of partial differential equations. For this reason, the adaptive procedure starts only after the spline-based reconstruction has finished computing a first approximation of the solution on an equidistant grid using the original algorithm of John et al. (2007), which does not require any starting guess. The newly developed adaptive algorithm consists of the following steps:

1. *Compute the second-order derivative of the current approximation*: The key observation for choosing the initial nodes of the adaptive grid is that, if $f(t, x)$ changes the sign of its curvature quickly, as at narrow peaks, then it is not possible to represent this region with a cubic function in one interval. This is because a cubic function can lead only to one single change of the sign of the curvature in one interval. In fact, the original algorithm always leads to very bad results if more than one change of the sign of the curvature of $f(t, x)$ occurs in one sub-interval (see for instance later Fig. 7). For this reason, we decided to place nodes at all points where the second-order derivative of the current reconstruction either changes its sign from a positive to a negative value, or vice versa.

2. *Compute the first-order derivative of the current approximation*: Nodes are also placed in those sub-regions where the absolute value of the first-order derivative is large, i.e., where the solution is steep. This idea resembles the well-known gradient indicator in adaptive methods for partial differential equations. For choosing the next nodes of the adaptive grid, the first-order derivatives of the spline at the nodes of the current grid are thus evaluated. The obtained values are ordered with respect to their size (absolute value) and then grouped into so-called windows. The default number of windows is set to be equal to the number of nodes that need to be chosen. In the first window all the points with the largest derivative values are gathered. All node points in a window are considered to be of the same importance. Starting with the first window, the algorithm picks up the points from left to right, in the increasing $x$ direction and accepts within the new list of nodes only those that have a minimal prescribed distance from the nearest node. Excessive clustering of nodes is avoided in this way. This procedure is applied until the appropriate total number of nodes has been obtained, which is given by the order of the spline and the number of known moments.

3. *Enlarge the domain*: Numerical tests have shown that it is useful to slightly enlarge at first the range identified by the original, equidistant algorithm of John et al. (2007) and to compute iteratively a new domain with the adaptively distributed nodes. For this purpose, the coordinate of the node $x_{n+1}$ is multiplied in practice by 1.2 (20% increase).

4. Go to step 1 of the original algorithm using the new distribution of the nodes.

Now, the original algorithm of John et al. (2007) is performed again. After this, a new distribution of the nodes is computed with the adaptive procedure, and so on. For all the cases presented in this paper, three node redistributions have been required at most before finding the final solution.

An approximation $f^{(k-1)}$ is considered to be the final approximation of $f(t, x)$ if:

- the error associated with all moments is sufficiently small

$$\max_{i=0,\ldots,L-1} |\text{relative error in } i\text{th moment of } f^{(k-1)}| < tol,$$

- and the approximation on the next adaptive grid leads to a growing mean error

$$\sum_{i=0}^{L-1} |\text{relative error in } i\text{th moment of } f^{(k-1)}|$$
$$\leq \sum_{i=0}^{L-1} |\text{relative error in } i\text{th moment of } f^{(k)}|.$$

The window approach described in step 2 does not select the nodes strictly with respect to the absolute value of their first-order derivative. Instead, the selection occurs within the windows from left to right (increasing $x$-direction). In our numerous tests, this approach has been found to lead to more accurate results, compared with a selection based only on the magnitude of the first-order derivative. This is due to the fact that the reconstructed function, being bounded on the left-hand boundary, usually tends to be slightly shifted to the right (larger $x$-values) compared with reality. The employed windows favor the left-hand side (lower $x$-value) and thus counterbalance this issue to some extent.

The workflow of the adaptive spline-based reconstruction algorithm is presented in Fig. 1.

## 3. Results and discussion

Using equidistant grids, the original algorithm has already shown excellent results for smooth distributions with a slowly changing sign of the PSD curvature (John et al., 2007). Therefore, we concentrate here on the cases from John et al., 2007 where the reconstruction was not really successful (second and fourth examples, called Examples 2.2 and 2.4 in the original paper).

The engineering background and the data (values of all moments) for all these test cases can be found in John et al. (2007). Similar to John et al. (2007), the adaptive algorithm has been implemented as a MATLAB script. The number of iterations needed to get the final distribution depends of course on the example considered and on the number of known moments. However, the computation time was less than 120 s on a standard PC for all simulations carried out up to now, including a graphical representation of all intermediate solutions. If necessary, this duration could be tremendously reduced by suppressing graphical outputs, writing a dedicated code instead of using MATLAB, optimizing further the algorithm and using a faster computer. This would finally allow the use of this approach for process control which is a major issue of chemical engineering (Rodrigo et al., 2004; Sundmacher et al., 2005; Agachi et al., 2007).

### 3.1. Multi-peak, smooth distributions

Figs. 2–6 present a comparison of the results obtained with the original (equidistant) and the adaptive algorithm for the smooth distribution with two peaks (Example 2.2 of John et al., 2007), one of them being considerably narrower than the other one. The reference distribution has been obtained numerically by solving directly the full Population Balance Equations. Such a distribution with two peaks is typical of crystallization applications, for which seeds are employed initially, so that finally both seed crystals and newly nucleated crystals will be found at different sizes. Our group is particularly interested in enantiomer crystallization. More information on that topic can be found for example in Qamar et al. (2006), or for a more general picture in Lorenz et al. (2006).

As already shown in John et al. (2007), the original approach is not able to resolve the changing sign of the curvature for the first, narrow peak and thus leads globally to a poor result. The adaptive algorithm is in most cases able to find suitable positions for the nodes, leading to an excellent reconstruction of the reference distribution.

As explained in the introduction, only a limited number of moments are usually known. It is therefore important to check how many moments are really needed for a good reconstruction of the PSD. For this purpose, a systematic study showing the results for three up to seven moments is presented.

Visually, results obtained with four to seven moments (documented respectively in Figs. 3–6) can be considered as good to very good (see for instance Fig. 6). On the other hand, the reconstruction using just three moments does not resolve the peaks with high precision. This is due to the lack of information when using such a small number of moments.

A quantitative evaluation of the reconstruction quality is presented in Table 1 (standard algorithm) and Table 2 (adaptive algorithm). Different methods and parameters have been used in order to quantify precisely the quality of the reconstruction. First, the norm of the global error is defined as

$$\text{Norm} = \frac{\int_0^{x_{\max}} |f_{reconst}(x) - f_{ref}(x)| dx}{\int_0^{x_{\max}} |f_{ref}(x)| dx}.$$
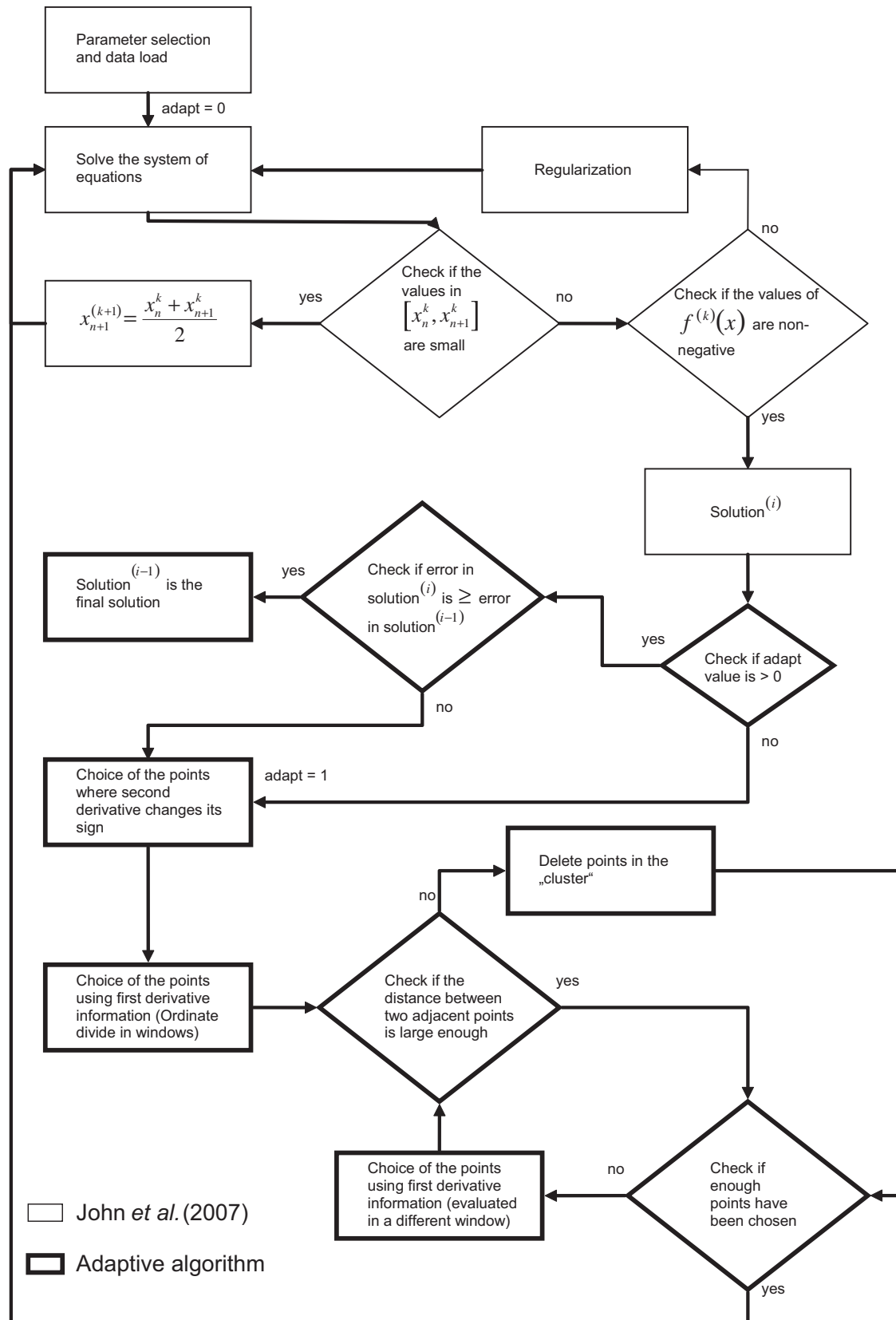
**Fig. 1.** Workflow of the adaptive spline-based reconstruction algorithm.

The correlation coefficient (Corr) between the reconstructed and the reference curve is furthermore computed using the built-in MATLAB function *corrcoef*.

For many practical purposes, the position and the height of the peaks observed in the PSD are essential pieces of information. Consequently, measuring the accuracy of the procedure for both
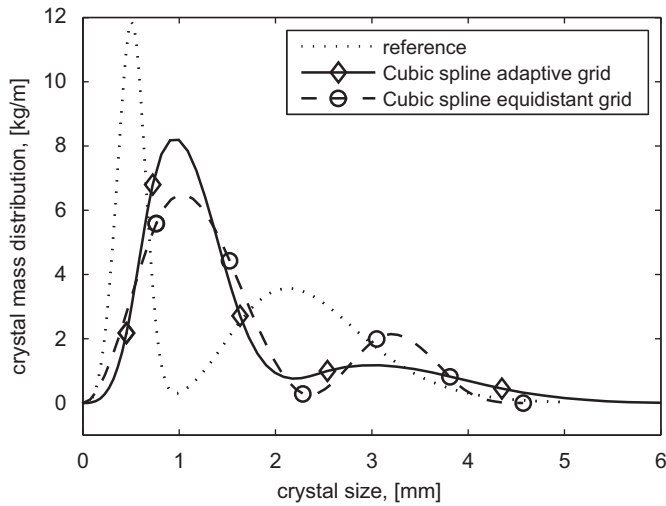
**Fig. 2.** Reconstruction of a two-peak distribution, comparison of equidistant and adaptive algorithm using three known moments.
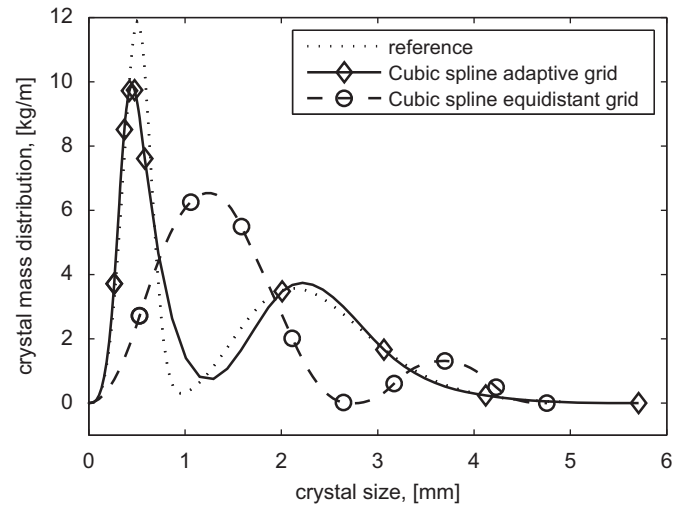


**Fig. 5.** Reconstruction of a two-peak distribution, comparison of equidistant and adaptive algorithm using six known moments.
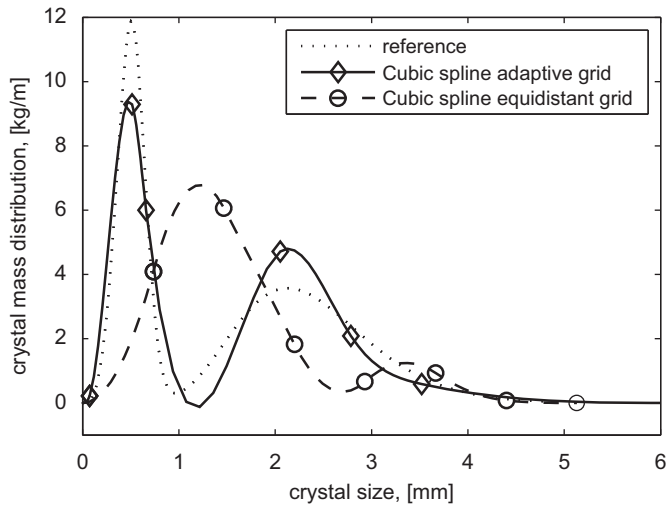


**Fig. 3.** Reconstruction of a two-peak distribution, comparison of equidistant and adaptive algorithm using four known moments.
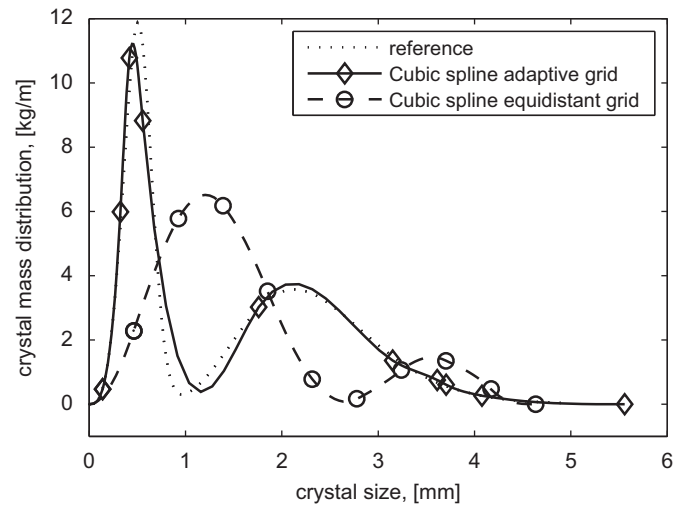


**Fig. 6.** Reconstruction of a two-peak distribution, comparison of equidistant and adaptive algorithm using seven known moments.
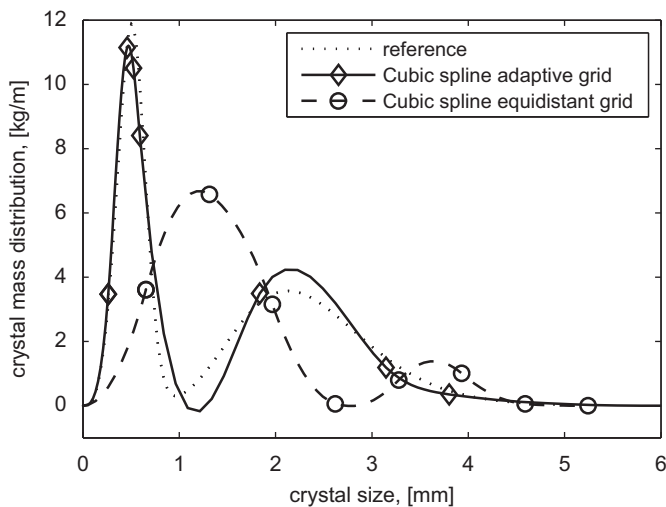


**Fig. 4.** Reconstruction of a two-peak distribution, comparison of equidistant and adaptive algorithm using five known moments.

**Table 1**

Quantitative evaluation of the smooth distribution reconstruction using the standard algorithm.

| Case | Norm (%) | Corr (%) | Negat (%) | | $\Delta H_{rel}$ (%) | $\Delta L_{rel}$ (%) |
|---|---|---|---|---|---|---|
| 3 mom | 95.8 | 17.8 | 0 | Left peak | 43.8 | 11.6 |
| | | | | Right peak | 38.2 | 21.2 |
| 4 mom | 98.8 | 9.3 | 0 | Left peak | 41.3 | 14.8 |
| | | | | Right peak | 64.3 | 24.8 |
| 5 mom | 107.6 | 9.5 | 0.14 | Left peak | 42.1 | 14.8 |
| | | | | Right peak | 60.4 | 29.4 |
| 6 mom | 104.9 | 12.1 | 0 | Left peak | 43.4 | 14.2 |
| | | | | Right peak | 62.3 | 31.4 |
| 7 mom | 102.5 | 13.2 | 0 | Left peak | 43.5 | 14.0 |
| | | | | Right peak | 58.1 | 27.8 |

quantities is also interesting, even if they do not describe the quality of the whole reconstruction. The corresponding errors are defined in the following equations:

Relative height difference ($\Delta H_{rel}$):

$$\Delta H_{rel} = \frac{|f_{reconst}(x_{peak,reconst}) - f_{ref}(x_{peak,ref})|}{|f_{ref}(x_{peak,ref})|}.$$

Relative position difference ($\Delta L_{rel}$):

$$\Delta L_{rel} = \frac{|x_{peak,reconst} - x_{peak,ref}|}{x_{max}}.$$

The relative negativity

$$Negat = \frac{min(f_{reconst})}{max(f_{reconst})}$$

has also been quantified, since in some cases slightly negative values allow to obtain much better reconstructions. It is interesting to know how much this will affect the results.

It can be seen clearly in Table 1 that the original algorithm of John et al. (2007) using an equidistant grid cannot produce the right solution. Even when considering more and more moments, the reconstruction quality does not increase measurably.

On the other hand, the adaptive algorithm (Table 2) fully exploits the supplementary information. With only three moments, the reconstruction is inaccurate. But, for four and more moments, the reconstruction quality is good up to excellent. Using more moments, the reconstruction quality increases further, but only slightly since the solution obtained with four moments is already good.

The moments obtained with the equidistant grid and the adaptive algorithm are compared with the moments of the initial test distribution in Tables 3 and 4. Reconstructions computed on the adaptive grids lead to very accurate moments, with relative errors lying below 1% for all moments considered. In contrast, the equidistant grid yields distributions with very small errors in the first two moments but sometimes large errors for higher moments (up to 15%).

**Table 2**
Quantitative evaluation of the smooth distribution reconstruction using the adaptive algorithm.

| Case | Norm (%) | Corr (%) | Negat (%) | | $\Delta H_{rel}$ (%) | $\Delta L_{rel}$ (%) |
|---|---|---|---|---|---|---|
| 3 mom | 107.1 | 5.0 | 0 | Left peak | 27.6 | 9.9 |
| | | | | Right peak | 67.3 | 19.0 |
| 4 mom | 19.0 | 96.9 | 0.52 | Left peak | 5.3 | 2.2 |
| | | | | Right peak | 21.9 | 1.4 |
| 5 mom | 17.2 | 97.8 | 0.73 | Left peak | 12.9 | 1.8 |
| | | | | Right peak | 11.2 | 1.8 |
| 6 mom | 16.2 | 96.5 | 0 | Left peak | 5.6 | 1.0 |
| | | | | Right peak | 4.8 | 1.8 |
| 7 mom | 12.8 | 97.2 | 0 | Left peak | 1.3 | 1.3 |
| | | | | Right peak | 3.9 | 0.8 |

**Table 3**
Comparison of the moments of the equidistant grid reconstruction with the initial test distribution (two-peak smooth distribution).

| Moments | Rel. error (%) | | | | |
|---|---|---|---|---|---|
| | 3 moments | 4 moments | 5 moments | 6 moments | 7 moments |
| $\mu_0$ | 4.66e − 6 | 3.76e − 6 | 2.78e − 6 | 1.69e − 6 | 1.44e − 6 |
| $\mu_1$ | 1.18e − 2 | 1.25e − 2 | 9.46e − 3 | 7.89e − 3 | 7.42e − 3 |
| $\mu_2$ | 1.02e + 1 | 1.16e + 1 | 8.47 | 7.23 | 7.15 |
| $\mu_3$ | | 1.18e + 1 | 9.37 | 6.70 | 7.34 |
| $\mu_4$ | | | 3.00 | 9.42e − 1 | 1.48 |
| $\mu_5$ | | | | 1.21e + 1 | 6.90 |
| $\mu_6$ | | | | | 1.50e + 1 |

### 3.2. Non-smooth distributions

The second example considers a non-smooth distribution with two peaks (John et al., 2007, Example 2.4). The first peak is extremely narrow and drops suddenly from its maximal value to zero. This distribution corresponds again to a preferential crystallization process, described in more details in Elsner et al. (2005).

The original algorithm on an equidistant grid completely fails for this application, as already shown in John et al. (2007). On the other hand, Fig. 7 demonstrates that the adaptive algorithm is able to give a rather good reconstruction for this very difficult case. The height and the position of both peaks are reproduced with good precision and even the steep gradient at the end of the first peak is relatively well resolved. The price to pay for this good resolution is a slightly negative value of the PSD for a short range behind the sharp peak. Since splines are intrinsically smooth functions, it cannot be expected that they will allow directly an exact description of a non-smooth PSD. This drawback is however in practice of minor importance compared with a correct estimation of the peak magnitudes and positions.

The quality of the reconstruction is quantified in Table 5. The comparison shows again the clear improvement of all indicators when using the adaptive algorithm. This shows that the adaptive spline-based reconstruction algorithm described in Section 2 is also able to automatically take into account a local non-smooth behavior of the distribution to reconstruct.

A quantitative comparison of the moments obtained with the reconstruction algorithms is shown for the non-smooth distribution in Table 6. The relative errors are below 1% for all moments

**Table 4**
Comparison of the moments of the adaptive algorithm reconstruction with the initial test distribution (two-peak smooth distribution).

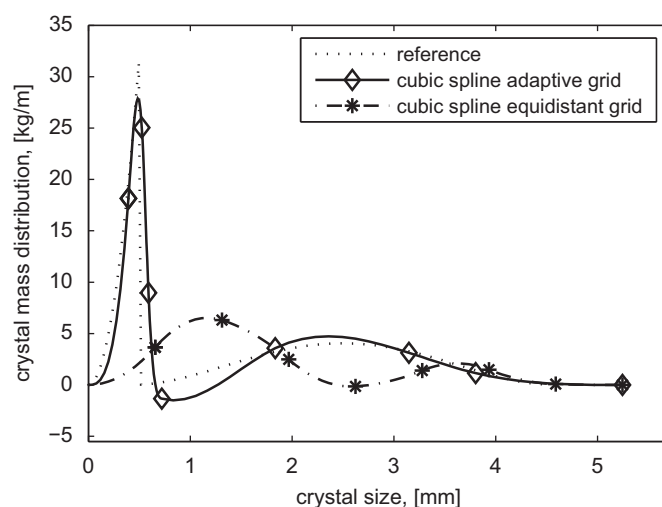| Moments | Rel. error (%) | | | | |
|---|---|---|---|---|---|
| | 3 moments | 4 moments | 5 moments | 6 moments | 7 moments |
| $\mu_0$ | 8.06e − 2 | 6.68e − 1 | 2.84e − 1 | 3.71e − 1 | 4.22e − 1 |
| $\mu_1$ | 2.66e − 2 | 4.98e − 1 | 1.57e − 1 | 2.52e − 1 | 2.45e − 1 |
| $\mu_2$ | 1.80e − 1 | 3.52e − 1 | 1.42e − 1 | 1.73e − 1 | 1.10e − 1 |
| $\mu_3$ | | 4.15e − 1 | 2.41e − 1 | 2.04e − 1 | 1.13e − 1 |
| $\mu_4$ | | | 4.22e − 1 | 3.14e − 1 | 1.95e − 1 |
| $\mu_5$ | | | | 5.63e − 1 | 3.18e − 1 |
| $\mu_6$ | | | | | 4.71e − 1 |



**Fig. 7.** Reconstruction of a two-peak distribution with steep gradient using five moments, comparison of equidistant and adaptive algorithm.

**Table 5**
Quantitative evaluation of the non-smooth distribution reconstruction using five moments.

| Case | Norm (%) | Corr (%) | Negat (%) | | $\Delta H_{rel}$ (%) | $\Delta L_{rel}$ (%) |
|---|---|---|---|---|---|---|
| Standard | 135.3 | 19.1 | 9.5 | Left peak | 69.4 | 16.9 |
| | | | | Right peak | 35.4 | 31.5 |
| Adaptive | 35.7 | 80.2 | 5.3 | Left peak | 11.0 | 0.2 |
| | | | | Right peak | 16.8 | 2.9 |

**Table 6**
Comparison of the moments of the reconstruction based on the equidistant grid and adaptive algorithms with the initial test distribution (non-smooth distribution).

| Moments | Rel. error (%) equidistant grid | Rel. error (%) adaptive algorithm |
|---|---|---|
| $\mu_0$ | 3.14e − 6 | 1.21e − 1 |
| $\mu_1$ | 1.00e − 2 | 4.11e − 1 |
| $\mu_2$ | 8.21 | 4.20e − 1 |
| $\mu_3$ | 7.04 | 1.42e − 1 |
| $\mu_4$ | 9.07e − 1 | 2.73e − 1 |

when using an adaptive grid, leading to a much better approximation compared with the equidistant grid algorithm.

### 3.3. Robustness of the reconstruction

As already explained in the introduction, the developed reconstruction process must be as robust as possible. When considering experimental measurements, the uncertainty is not negligible. It must be checked that the predicted distribution is not impacted too strongly by such inaccurate inputs.

Even when considering results of numerical simulations, the shape and extent of the distribution are usually very poorly known at first. Therefore, the reconstruction must be able to work efficiently with a very low level of starting information.

Both issues have been checked separately, first by modifying the input moments by a certain percentage, thus mimicking a possible (measurement) error. In a second step, the size of the (guessed) initial domain has been varied over an order of magnitude, in order to quantify its impact.

The effect of an error in the moments has been first investigated. Systematic as well as random errors have been introduced in the original moments and the final distribution obtained can be seen in Figs. 8 and 9, respectively.

When considering systematic errors, all moments are modified by multiplying or dividing them with the same factor, e.g. 1.3 for 30% relative error. As demonstrated in Fig. 8, such systematic errors fortunately do not have a very large impact on the reconstruction. Even when a large relative error of 30% is applied, the shape of the distribution remains very similar and the position of the peaks is still very well predicted (Table 7). This is undoubtedly related to the fact that the coupling between function and moments (Eq. (1)) is linear.

Random errors have a larger impact on the shape of the distribution (Fig. 9). For random errors, each moment is again multiplied or divided by the same factor (e.g. 1.1 for 10% relative error), but a random process is called to decide for each moment individually if a multiplication or a division should take place. As a consequence, some moments will be increased while some others are reduced in a random manner.

Here also, the adaptive algorithm has been able to deliver a reconstruction of acceptable quality (Table 8). In fact, the
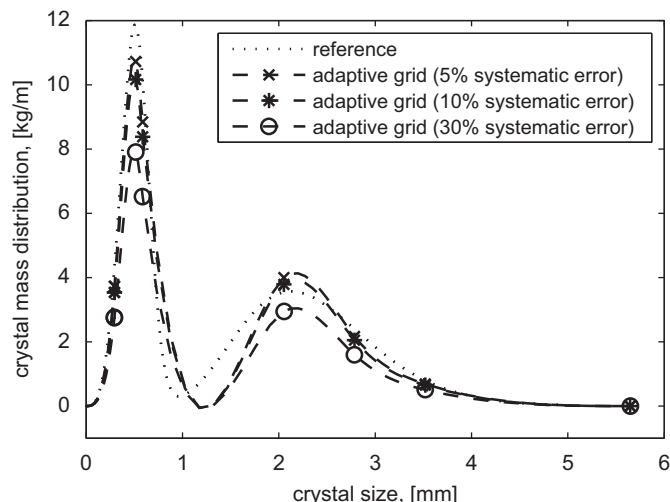


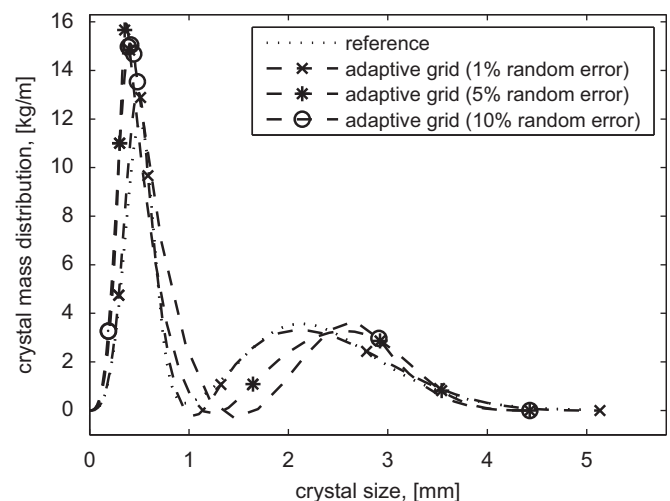**Fig. 8.** Reconstruction of a two-peak distribution using four moments with systematic error.



**Fig. 9.** Reconstruction of a two-peak distribution using four moments with random error.

**Table 7**
Quantitative evaluation of the reconstruction using four moments with systematic error.

| Case | Norm (%) | Corr (%) | Negat (%) | | $\Delta H_{rel}$ (%) | $\Delta L_{rel}$ (%) |
|---|---|---|---|---|---|---|
| 5% syst. error | 21.0 | 95.4 | 0 | Left peak | 15.3 | 0.2 |
| | | | | Right peak | 4.8 | 2.8 |
| 10% syst. error | 23.4 | 95.3 | 0 | Left peak | 19.8 | 0.2 |
| | | | | Right peak | 9.8 | 2.8 |
| 30% syst. error | 38.2 | 95.3 | 0 | Left peak | 37.7 | 0.2 |
| | | | | Right peak | 29.8 | 2.8 |

algorithm works indeed very well and delivers the correct moments with a very high accuracy. The observed discrepancies are directly connected to the random modification of the moments. Even a small change in the moments leads to a considerably different distribution. This illustrates the need for an accurate determination of the moments. The needed level of accuracy certainly constitutes a real challenge, in particular for experimental measurements.

**Table 8**
Quantitative evaluation of the reconstruction using four moments with random error.

| Case | Norm (%) | Corr (%) | Negat (%) | | $\Delta H_{rel}$ (%) | $\Delta L_{rel}$ (%) |
|---|---|---|---|---|---|---|
| 1% random error | 9.6 | 99.3 | 1.69 | Left peak | 10.9 | 0.2 |
| | | | | Right peak | 7.6 | 1.6 |
| 5% random error | 41.3 | 87.4 | 8.36 | Left peak | 34.3 | 2.7 |
| | | | | Right peak | 8.1 | 9.8 |
| 10% random error | 56.6 | 85.3 | 19.87 | Left peak | 26.8 | 1.7 |
| | | | | Right peak | 3.4 | 12.2 |

**Table 9**
Robustness test regarding the choice of the initial interval.

| Initial guess (mm) | Final domain (mm) | Norm error (%) | Corr (%) |
|---|---|---|---|
| 5 | 4.643 | 28.3 | 94.1 |
| 6 | 5.765 | 28.4 | 90.0 |
| 8 | 5.238 | 27.2 | 88.3 |
| 10 | 5.645 | 19.0 | 96.9 |
| 12 | 5.424 | 21.1 | 93.1 |
| 30 | 4.805 | 30.5 | 91.4 |
| 50 | 5.954 | 42.1 | 79.0 |
| 90 | 9.047 | 38.8 | 87.2 |

In a second step, the size of the initial domain has been slowly increased by more than an order of magnitude considering again the smooth two-peak distribution. The really useful domain for this distribution extends up to 5 mm. The adaptive reconstruction process has been carried out with an initial guess of 5, 6, 8, 10, 12, 30, 50, and 90 mm. The final domain identified by the procedure and the resulting global errors are shown in Table 9. These tests have shown that, as long as a few points are present during the first iteration within the real domain of interest, the adaptive procedure will be able to converge to the right region. The best result is obtained when choosing as a first guess twice the size of the real domain of interest.

Altogether, the reconstructions obtained with the adaptive algorithm are of a much better quality and considerably more robust than the original results using an equidistant grid for all configurations tested up to now, without any exception.

## 4. Conclusions and outlook

This paper presents a considerable improvement of an algorithm suitable for reconstructing a PSD knowing only a small number of its moments by using splines. The original algorithm from John et al. (2007) failed to reconstruct distributions with a quickly changing curvature or with local non-smooth behavior. To overcome these problems, an adaptive grid has been introduced, allowing a much more appropriate resolution of critical regions, through an iterative analysis of the first and second-order derivatives of the intermediate solutions. It has been demonstrated that the adaptive algorithm leads to reconstructions with a much better accuracy than the equidistant grid approach. The needed computing time is still very small (expressed in seconds, without optimizing the process), so that it would be probably possible to use this algorithm for process control.

The numerous tests carried out during the development of this procedure reveal following features:

- For a really accurate reconstruction of a two-peak, smooth distribution, four moments should be known. A reconstruction with only three moments is already possible, but will lead only to a semi-quantitative description.
- It is not necessary to know the domain of the function to reconstruct with a high precision. A first guess with only the right order of magnitude (i.e., knowing only the typical size of the largest particles) is fully sufficient to start the process. A good initial guess is twice the real domain of interest, if known in advance.
- When more moments are known, the accuracy of the reconstruction increases as expected.
- To reconstruct accurately a non-smooth distribution, more moments are needed than for a smooth distribution. As a rough recommendation, one moment more should be known for each non-smooth event compared with a smooth distribution with the same number of peaks.
- The reconstruction process is robust enough to tolerate some error in the moment values. Nevertheless, these errors must of course be minimized, since a random error of 10% might already lead in reality to a considerably different distribution.

Future work will consider the extension of the spline-based reconstruction algorithm to bivariate distributions.

The MATLAB script for the original algorithm is freely available under the Web page http://www.uni-magdeburg.de/isut/LSS, Menu "Downloads". The script of the new, adaptive algorithm will become also freely available under the same address, simultaneously with the release of the present publication.

## Appendix A. On the unique reconstruction of a PSD if all moments are known

This appendix shows that in the framework considered in this paper, a function can be uniquely reconstructed if all its moments are known. This is in general not possible without appropriate conditions, see the examples by White (1990) and McGraw et al. (1998).

As emphasized in the introduction, a PSD $f(x)$ is defined in practice over a bounded interval $[a,b]$, $0 < a < b < \infty$. We assume that $f \in L^2(a,b)$, where $L^2(a,b)$ is the Lebesgue space of square-integrable functions on $(a,b)$. This assumption is realistic, e.g. sufficient conditions for $f \in L^2(a,b)$ are that $f(x)$ is bounded in $(a,b)$ or that $f(x)$ is continuous in $[a,b]$. The result of the spline-based reconstruction algorithm is by construction a continuous function in $[a,b]$.

Let us assume that there are different distributions $f, g \in L^2(a,b)$ such that

$$\int_a^b x^k f(x)\,dx = \int_a^b x^k g(x)\,dx, \quad k = 0, 1, 2, \ldots \ . \tag{2}$$

It is well known that the system of Legendre polynomials $\{P_0(x), P_1(x), P_2(x), \ldots\}$ is an orthogonal basis of $L^2(a,b)$, i.e. it holds

$$\int_a^b P_i(x)P_j(x)\,dx = \begin{cases} A_i > 0, & i = j, \\ 0 & \text{else}. \end{cases} \qquad (3)$$

Since the Legendre polynomials form a basis, there are unique representations of the form

$$f(x) = \sum_{i=0}^{\infty} \alpha_i P_i(x), \quad g(x) = \sum_{i=0}^{\infty} \beta_i P_i(x), \quad \alpha_i, \beta_i \in \mathbb{R}.$$

In addition, the monomial of order $k$ can be represented as a linear combination of the Legendre polynomials $P_0, \ldots, P_k$,

$$x^k = \sum_{i=0}^{k} \gamma_i P_i(x), \quad \gamma_i \in \mathbb{R} \quad \text{with } \gamma_k \neq 0.$$

Let Eq. (2) hold for $k=0$, i.e.

$$0 = \int_a^b (f(x)-g(x))\,dx = \int_a^b \sum_{i=0}^{\infty} (\alpha_i - \beta_i)P_i(x)\,dx = \sum_{i=0}^{\infty}(\alpha_i - \beta_i)\int_a^b P_i(x)\,dx.$$

Since $P_0(x) = C \in \mathbb{R}$, it holds with Eq. (3)

$$\int_a^b P_i(x)\,dx = \begin{cases} A_0 > 0, & i = 0, \\ 0 & \text{else}. \end{cases}$$

Hence, $0 = (\alpha_0 - \beta_0)A_0$ from what $\alpha_0 = \beta_0$ can be deduced.

Now, the argument continues by induction. Let $\alpha_i = \beta_i$ for $i = 0, 1, \ldots, k-1$. Using this condition, one obtains

$$0 = \int_a^b x^k(f(x)-g(x))\,dx$$

$$= \int_a^b \left(\sum_{j=0}^{k} \gamma_j P_j(x)\right)\left(\sum_{i=0}^{\infty}(\alpha_i - \beta_i)P_i(x)\right)dx$$

$$= \int_a^b \left(\sum_{j=0}^{k} \gamma_j P_j(x)\right)\left(\sum_{i=k}^{\infty}(\alpha_i - \beta_i)P_i(x)\right)dx.$$

Multiplication of the sums gives terms of the form

$$\int_a^b P_j(x)P_i(x)\,dx, \quad j = 0, \ldots k \quad \text{and} \quad i = k, k+1, \ldots.$$

According to Eq. (3), these integrals are only non-zero if $i = j(=k)$. Hence, it follows

$$0 = \int_a^b \gamma_k P_k(x)(\alpha_k - \beta_k)P_k(x)\,dx = \gamma_k(\alpha_k - \beta_k)A_k.$$

Since $A_k > 0$ and $\gamma_k \neq 0$, one obtains $\alpha_k = \beta_k$. Hence $\alpha_i = \beta_i$, $i = 0, 1, 2, \ldots$, and the basis property of the Legendre polynomials finally yields $f(x) = g(x)$.

The examples on non-unique reconstructions from White (1990) and McGraw et al. (1998) are defined on infinite intervals $I$. In this case, polynomials do not belong to $L^2(I)$ and consequently there is no polynomial basis of $L^2(I)$.

## References

Abramov, R.V., 2007. An improved algorithm for the multidimensional moment-constrained maximum entropy problem. Journal of Computational Physics 226, 621–644.

Agachi, P.Ş., Nagy, Z.K., Cristea, M.V., Imre-Lucaci, Á., 2007. Model Based Control: Case Studies in Process Engineering. Wiley-VCH, Weinheim.

Allen, T., 1997. Particle Size Measurement. Particle Technology Series, fifth ed. Springer, Berlin.

Alopaeus, V., Laakkonen, M., Aittamaa, J., 2008. Solution of population balances by high order moment-conserving method of classes: reconstruction of a non-negative density distribution. Chemical Engineering Science 63, 2741–2751.

Bałdyga, J., Orciuch, W., 2001. Barium sulphate precipitation in a pipe: an experimental study and CFD modelling. Chemical Engineering Science 56, 2435–2444.

Bandyopadhyay, K., Bhattacharya, K., Biswas, P., Drabold, D.A., 2005. Maximum entropy and the problem of moments: a stable algorithm. Physical Review E 71 057701-1–057701-4.

Diemer, R., Olson, J., 2002. A moment methodology for coagulation and breakage problems: part 2-moment models and distribution reconstruction. Chemical Engineering Science 57, 2211–2228.

Elsner, M., Menéndez, D.F., Muslera, E., Seidel-Morgenstern, A., 2005. Experimental study and simplified mathematical description of preferential crystallization. Chirality 17, 183–195.

Fan, R., Marchisio, D., Fox, R., 2004. Application of the direct quadrature method of moments to polydisperse gas-solid fluidized beds. Powder Technology 139, 7–20.

John, V., Angelov, I., Öncül, A.A., Thévenin, D., 2007. Techniques for the reconstruction of a distribution from a finite number of its moments. Chemical Engineering Science 62, 2890–2904.

Kass, R.E., Wasserman, L., 1996. Selection of prior distributions by formal rules. Journal of the American Statistical Association 91, 1343–1370.

Lorenz, H., Perlberg, A., Sapoundjiev, D., Elsner, M., Seidel-Morgenstern, A., 2006. Crystallization of enantiomers. Chemical Engineering and Processing 45, 863–873.

Marchisio, D., Barresi, A., Garbero, M., 2002. Nucleation, growth and agglomeration in barium sulfate turbulent precipitation. A.I.Ch.E. Journal 48, 2039–2050.

Marchisio, D., Fox, R., 2005. Solution of population balance equations using the direct quadrature method of moments. Journal of Aerosol Science 36 (1), 43–73.

McGraw, R., Nemesure, S., Schwatz, S., 1998. Properties and evolution of aerosols with size distributions having identical moments. Journal of Aerosol Science 29 (7), 761–772.

Mersmann, A., 2001. Crystallization Technology Handbook, second ed. Marcel Dekker, Inc., New York.

Öncül, A.A., Janiga, G., Thévenin, D., 2009. Comparison of various micromixing approaches for computational fluid dynamics simulation of barium sulfate precipitation in tubular reactors. Industrial & Engineering Chemistry Research 48, 999–1007.

Qamar, S., Elsner, M., Angelov, I., Warnecke, G., Seidel-Morgenstern, A., 2006. A comparative study of high resolution schemes for solving population balances in crystallization. Computers & Chemical Engineering 30, 1119–1131.

Rodrigo, A., Lorenz, H., Seidel-Morgenstern, A., 2004. Online monitoring of preferential crystallization of enantiomers. Chirality 16, 499–508.

Scales, J.A., Tenorio, L., 2001. Prior information and uncertainty in inverse problems. Geophysics 66, 389–397.

Schwarzer, H., Schwertfirm, F., Manhart, M., Schmidt, H.-J., Peukert, W., 2006. Predictive simulation of nanoparticle precipitation based on the population balance equation. Chemical Engineering Science 61, 167–181.

Strumendo, M., Arastoopour, H., 2008. Solution of PBE by MOM in finite size domains. Chemical Engineering Science 63, 2624–2640.

Sundmacher, K., Kienle, A., Seidel-Morgenstern, A., 2005. Integrated Chemical Processes: Synthesis, Operation, Analysis, and Control. John Wiley & Sons, Weinheim.

Wei, H., Zhou, W., Garside, J., 2001. Computational fluid dynamics modeling of the precipitation process in a semibatch crystallizer. Industrial and Engineering Chemistry Research 40, 5255–5261.

White, W., 1990. Particle size distributions that cannot be distinguished by their integral moments. Journal of Colloid and Interface Science 135, 297–299.

Woodbury, A.D., 2004. A FORTRAN program to produce minimum relative entropy distributions. Computers and Geosciences 30, 131–138.

Wright, D.L., 2000. Retrieval of optical properties of atmospheric aerosols from moments of the particle size distribution. Journal of Aerosol Sciences 31, 1–18.